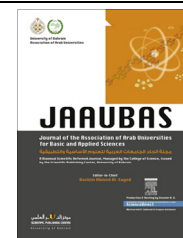




University of Bahrain
**Journal of the Association of Arab Universities for
Basic and Applied Sciences**

www.elsevier.com/locate/jaaubas
www.sciencedirect.com



ORIGINAL ARTICLE

Adsorption/desorption of Direct Yellow 28 on apatitic phosphate: Mechanism, kinetic and thermodynamic studies



H. El Boujaady ^{*}, M. Mourabet, M. Bennani-Ziatni, A. Taitai

Team Chemistry and Valorization of Inorganic Phosphates, Department of Chemistry, Faculty of Sciences, Ibn Tofail University, 13000 Kenitra, Morocco

Received 12 June 2013; revised 26 August 2013; accepted 29 September 2013
Available online 23 October 2013

KEYWORDS

Adsorption;
PTCa;
Desorption;
Decolourization;
Dye;
Kinetics

Abstract In this study, the adsorption potential of apatitic tricalcium phosphate for the removal of Direct Yellow 28 (DY28) from aqueous solution has been investigated by using batch mode experiments. The effects of different parameters such as pH, adsorbent dosage, initial dye concentration, contact time, addition of ions and temperature have been studied to understand the adsorption behavior of the adsorbent under various conditions. The adsorbent has been characterized by pHzpc measurement, chemical analyses, FTIR, XRD and TEM. The Langmuir and Freundlich models are found to be the best to describe the equilibrium isotherm data, with a maximum monolayer adsorption capacity of 67.02 mg g⁻¹. Thermodynamic parameters including the Gibbs free energy ΔG , enthalpy ΔH , and entropy ΔS have revealed that the adsorption of DY28 on the apatitic tricalcium phosphate is feasible, spontaneous and endothermic. Among the kinetic models tested for apatitic tricalcium phosphate, the pseudo-second-order model fits the kinetic data well. The introduction of orthophosphate ions in the medium causes a decrease of adsorption. The addition of Ca²⁺ ions favors the adsorption. The results of this study have demonstrated the effectiveness and feasibility of the apatitic tricalcium phosphate for the removal of DY28 from aqueous solution.

© 2013 Production and hosting by Elsevier B.V. on behalf of University of Bahrain.

1. Introduction

In Morocco the textile industry, represents 31% of all Moroccan industries whose reactive dyes are widely used for dyeing wool and nylon. The textile industry is one of the greatest generators of liquid effluent pollutants, due to the high quantities of water used in the dyeing processes. Textile wastewater is a

complex and highly variable mixture of many polluting substances including dye (Robinson et al., 2001). Many dyes and pigments contain aromatic rings in their structures, which make them toxic, non-biodegradable, carcinogenic and mutagenic for aquatic systems and human health (Lian et al., 2009).

A variety of methods have been employed for removing dyes from colored effluents, such as membrane filtration, oxidation, coagulation–flocculation, biological treatment, electrochemical process and adsorption (Zhang et al., 2013; Maezawa et al., 2007; Szygula et al., 2009; Khataee and Dehghan, 2011; Del Río et al., 2011; Dogan et al., 2007). Among these tech-

^{*} Corresponding author. Tel.: +212 671334031.

E-mail address: elboujaadyhicham@yahoo.fr (H. El Boujaady).

Peer review under responsibility of University of Bahrain.

niques, adsorption is a common technique used for dye removal from aqueous solution, mainly because it is relatively low in cost, robust, environmentally friendly and simple. A starting point in the development of an adsorption unit is the choice of an adsorbent among the various adsorbents.

Different kinds of adsorbents to remove dyes from aqueous solutions have been reported in the literature, such as untreated Coffee residues (Kyzas et al., 2012), activated palm ash (Hameed et al., 2007), Pine Cone (Mahmoodi et al., 2011), bamboo charcoal (Liao et al., 2012), peanut hull (Tanyildizi, 2011), chitosan (Iqbal et al., 2011), agricultural solid wastes (Mohd Salleh et al., 2011), sepiolite (Dogan et al., 2007), animal bone meal (El Haddad et al., 2012) and others.

Recently many researchers have proved the capability of calcium phosphate as adsorbents to remove many types of pollutants (Mourabet et al., 2011, 2012; El Boujaady et al., 2011; El Haddad et al., 2012, 2013). However, there is a lack of literature dealing with the possible application of apatitic tricalcium phosphate as adsorbents for dyes.

Nanocrystalline hydroxyapatite [$\text{Ca}_{10}(\text{PO}_4)_6(\text{OH})_2$, HAP] exhibits excellent biocompatibility and adsorption properties, and has been widely used as adsorbents for the adsorption and separation of biomolecules (Wei et al., 2009; Takagi et al., 2004), and for the removal of heavy metals, and phenol (Mobasherpour et al., 2012; Wei et al., 2010). The environmental risk of nanocrystalline HAP itself can be neglected because it has displayed good cytocompatibility (Lin et al., 2005). Moreover, calcium phosphate has also been used for the adsorption of amino acids (El Rhilassi et al., 2011, 2012). The present study was intended to remove Direct Yellow 28 (DY28) from aqueous solutions using apatitic prepared phosphate as a new cost adsorbent. The effect of various parameters like, adsorbent amount, dye concentration, contact time, pH and temperature, kinetics, equilibrium and thermodynamic studies was investigated. Furthermore the characterizations of PTCa have been done by using XRD analysis, Transmission electron microscopy (TEM) and energy dispersive X-ray (EDX) analysis, and FTIR spectroscopy.

2. Materials and methods

2.1. Adsorbent

Apatitic tricalcium phosphate (PTCa) was prepared at room temperature by a double decomposition method (Heughebaert, 1977). The solution A (47 g of calcium nitrate $\text{Ca}(\text{NO}_3)_2 \cdot 4\text{H}_2\text{O}$ (Scharlau, Spain) in 550 ml of distilled water + 20 ml of ammonia solution) was added quickly at room temperature into the solution B (26 g of di-ammoniumhydrogenphosphate $(\text{NH}_4)_2\text{HPO}_4$ (Riedel-de Haën, Germany) in 1300 ml of distilled water + 20 ml ammonia solution). The precipitate was filtered, washed, and dried at 353 K for 24 h.

2.2. Adsorbate

The Direct Yellow 28 (DY28) was obtained from a textile firm as a commercially available dye formulation and was used without further purification. It is a soluble dye in water due to the presence of solubilizing groups (SO_3Na). The structure and characteristics of this dye are illustrated in Table 1.

The dye (DY28) is a large molecule symmetrical consisting of an azo group, two groups benzothiazols and two solubilizing groups (SO_3Na). The solutions were prepared by dissolving the required amount of dye in distilled water. The concentration of the dye was determined at 396 nm, using UV spectrophotometer ("UV-2005", Selecta, Spain).

2.3. Experimental protocol

To study the kinetics of adsorption of the dye at 298 K, a volume of 10 ml of solution concentration 100 mg/L of dye was placed in contact with 200 mg of adsorbent in a test tube. The mixture was stirred at a constant speed (500 rpm) for one minute and then placed in a water bath at 298 K. Later, the solid was separated from the mother solution by filtration through a sintered glass and the dye concentration was determined using the UV-vis spectrophotometer.

The quantity of dye per which was fixed gram of adsorbent was given by the following equation:

$$Q_t = (C_0 - C_t)V/m \quad (1)$$

where Q_t is the quantity of dye in mg per gram of adsorbent, C_0 and C_t are respectively the initial concentrations and time t of the dye (mg/L), V : volume of solution (L), m : mass of adsorbent used (g). The percentage of dye removal was calculated from the relationship:

$$\% \text{ of dye removal} = (C_0 - C_t)/C_0 \quad (2)$$

C_0 and C_t are respectively the initial concentrations and at the time t of the dye (mg/L).

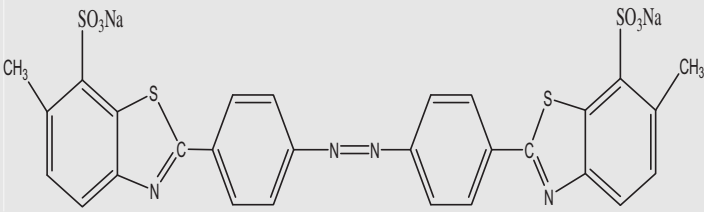
The effect of solid quantity on removal of Direct yellow 28 (DY28) was investigated in batch experiments by adding various amounts of adsorbent in the range of 50–400 mg powder into a test tube containing 10 ml of dye solution. The initial dye concentrations of the solutions were fixed at 100 mg/L, for all batch experiments. The suspension was then stirred for 1 min, after which time the solution was coagulated and settled and the supernatant was analyzed for the remaining dye.

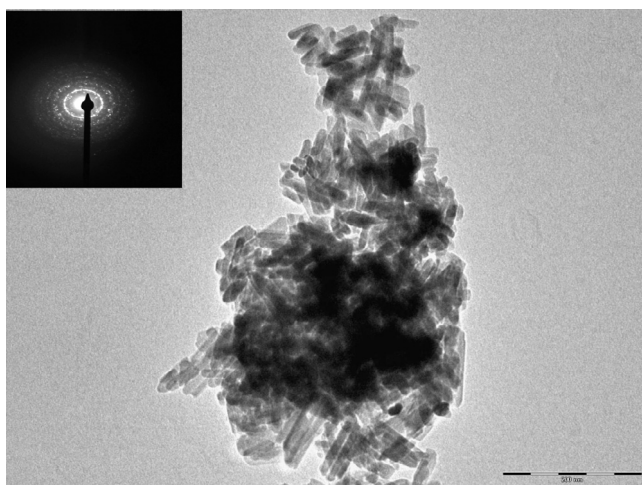
2.4. Characterization of the adsorbent

Calcium phosphate was characterized by chemical and physical analyses. The calcium content in the solid was determined by complexometry with EDTA and the phosphate ion content by spectrophotometry of phospho-vanado-molybdic acid. The specific surface area was determined according to the BET (Brunauer-Emmett-Teller) method using N_2 adsorption. Infrared spectroscopy IR was carried out after dispersion of anhydrous KBr (about 1 mg product to 100 mg of KBr) using VERTEX 70 spectrophotometer (Bruker Optics, Germany). Particle size and morphology of as-dried powders were determined by TEM Tecnai G² (Philips CM120, USA) observations. An X-ray Powder diffraction (XRD) pattern was analyzed using X'Pert PRO (Germany) X-ray diffractometer with Cu K radiation.

The pH of the zero point charge (pH ZPC) has been determined by placing 0.2 g of adsorbent in glass stopper bottle containing 20 ml of 0.01 M NaCl solutions. The initial pH of these solutions has been adjusted by either adding 0.1 M NaOH or 0.1 M HCl. The bottles have been placed in an

Table 1 Structure and characteristics of DY28.

Name	DY28 (C.I. Direct Yellow 28)
Chemical structure	
Molecular formula	C ₂₈ H ₁₈ N ₄ O ₆ S ₄ ·2Na
Other name	Disodium 5-(5-methyl-1,3-benzothiazol-2-yl)-2-[4-(5-methyl-1,3-benzothiazol-2-yl)-2-sulfonato-phenyl]azo-benzenesulfonate
Molecular weight (g/mol)	680.716

**Figure 1** TEM images and SAED patterns of as-dried samples of PTCa.

incubator shaker at 298 K for 24 h, and the final pH of supernatant has been measured. The $\Delta\text{pH} = \text{pH}(\text{final}) - \text{pH}(\text{initial})$ have been plotted against the initial pH, the pH at which ΔpH was zero was taken as a pH ZPC.

3. Results and discussion

3.1. Characterization of the adsorbent

Chemical analyses showed that Ca/P ratio was 1.5. The specific surface area of the synthetic apatite was 62 (m²/g). In Fig. 1 TEM image and SAED (selected area electron diffraction) patterns of all samples are presented. It resulted that sample are composed of needle-like nanoparticles of length 50–100 nm and width 8–20 nm. SAED pattern exhibited spotted sharp and continuous rings that evidence polycrystalline grains.

Fig. 2 illustrates the FTIR spectrums of the PTCa before adsorption (a) and PTCa after adsorption process. (b) The PTCa prepared shows characteristic bands of a tricalcium phosphate apatitic. On see bands PO₄³⁻ vibration groups in surrounding apatite located at 470.8, 565.8, 603.9, 962.6,

1028.6 and 1087 cm⁻¹. We also note the presence of characteristic bands of hydroxide ions OH⁻ at 634.8 cm⁻¹ and 3571.1 cm⁻¹. The band located at 876.7 cm⁻¹ associated with HPO₄²⁻ ions due to the stretching vibration of the link PO (H), confirms that it is a deficient apatite. The bands located at 1635.9 and 3137.1 cm⁻¹ (Bakan et al., 2013) are assigned to the vibration of the hydroxyl group in water.

The band located at 876.7 cm⁻¹ associated with HPO₄²⁻ ions, is found to be shifted to 875.8 cm⁻¹ after adsorption, this may be responsible for the chemical interaction of the DY28 with HPO₄²⁻ groups on the PTCa. The transmittance at wavenumber 3571.1 cm⁻¹ and 634.8 cm⁻¹ is found to be shifted to 3571.1 cm⁻¹ and 634.8 cm⁻¹ on adsorption, and no chemical interaction of the DY28 with O–H groups on the PTCa was observed. In addition, the transmittance at wavenumbers 470.8, 565.8, 603.9, 962.6 and 1028.6 cm⁻¹ is found to be shifted to 472.7, 566.1, 604.0, 962.6 and 1024.7 cm⁻¹, respectively on adsorption and this may be responsible for the chemical interaction of the DY28 with PO₄³⁻ groups on the PTCa. Therefore, from the above results, it can be concluded that HPO₄²⁻ and PO₄³⁻ groups are involved in the interaction between the apatitic phosphate and dye.

X-ray diffraction patterns of PTCa (Fig. 3a) showed reflections characteristic of poorly crystalline apatite, no other phase was detected. The overlapping reflections, indicated its low crystallinity. No structural changes of PTCa were detected by the powder X-ray diffraction analysis of the solid obtained after interaction of PTCa with dye solution (Fig. 3b). In addition; the intensity of XRD pattern was apparently lower than that of the original PTCa, which showed that the degree of crystallinity decreased after adsorption of dye. We attribute this to the fact that the dye molecules entered the crystalline region and interrupted its continuity.

The pHZPC of the PTCa was found to be 5.6 (Fig. 4). When pH is lower than 5.6, the surface of PTCa becomes positively charged and the opposite for pH values higher than 5.6, the surface becomes negatively charged.

3.2. Effect of solid quantity

Results are shown in Fig. 5. As indicated, 84.53% of DY28 were removed at the initial quantity of 0.05 g of PTCa. The removal of dye increased with increasing solid quantity up to

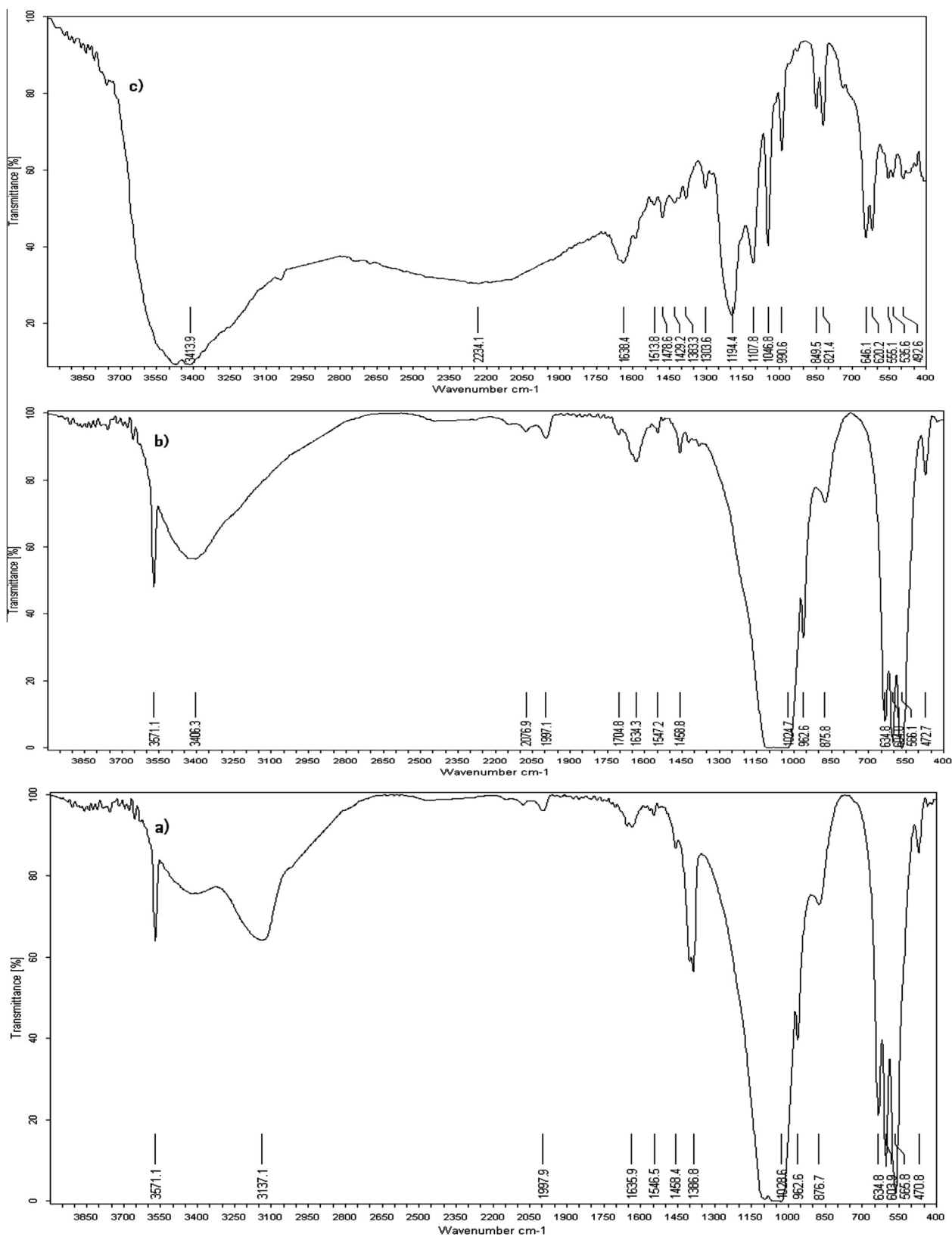


Figure 2 FTIR spectra: (a) PTCa before adsorption, (b) PTCa after adsorption of DY28 and (c) DY28.

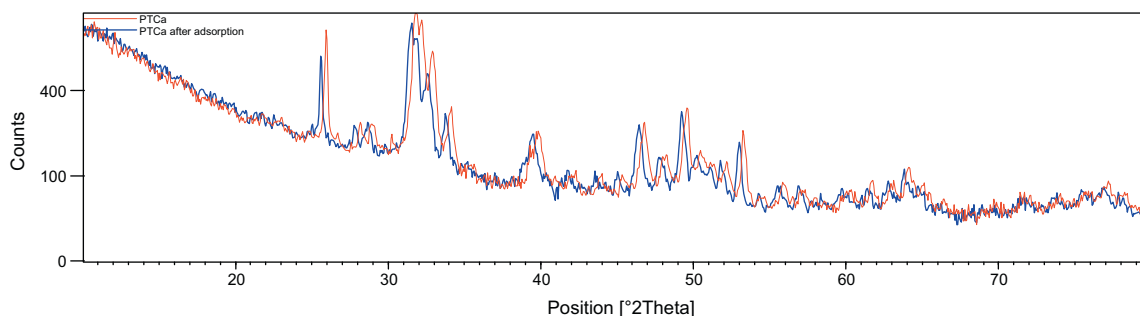


Figure 3 XRD patterns of (a) PTCa before adsorption and (b) PTCa after adsorption of DY28.

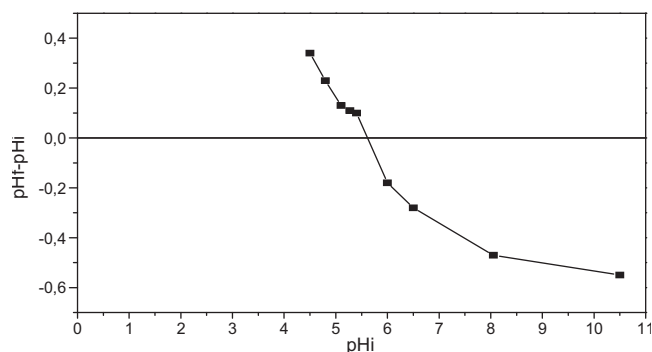


Figure 4 pHZPC of PTCa.

0.2 g and reached to 99.49% for PTCa, at this quantity. Hence, the optimum quantity of PTCa powder for removing DY28 was found to be 0.2 g and was used for further study.

3.3. Kinetics of adsorption

The equilibrium was quickly reached. The maximum adsorption of the dye was observed in the first half hour of contact. This fast rate can be explained by the high number of active sites available at the beginning of relative adsorption sites remaining after some time.

Fig. 6 presents the kinetic results of the adsorption process. The equilibrium was reached within a few minutes, by

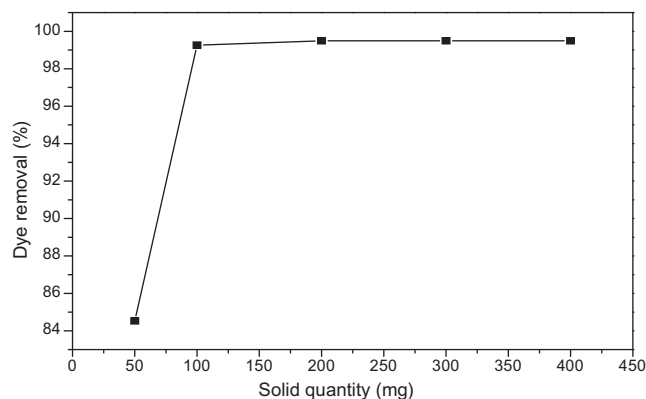


Figure 5 Effect of initial quantity of removal of DY28 on PTCa (initial dye concentration: 100 mg/L, initial pH, stirring time: 1 min, at 298 K, contact time: 6 h).

establishing a well-formed plateau, indicating also that the PTCa is a very effective adsorbent in a very short time for this textile dye.

Kinetic adsorption data were analyzed using the Lagergren pseudo-first-order kinetic model, the pseudo-second-order model and the intraparticle diffusion model.

The pseudo first order equation was represented by Lagergren (Lagergren, 1898).

$$\text{Log}(Q_e - Q_t) = \text{Log}(Q_e) - K_1/2.3t \quad (3)$$

The pseudo second order (Ho and McKay, 1999, 2000) model has been examined to find out the adsorption mechanism, for the pseudo second order rate constant K_2 is given by the following equation:

$$t/Q_t = 1/2K_2Q_e^2 + t/Q_e \quad (4)$$

For the second order rate constant K_3 is given by the following equation:

$$1/(Q_e - Q_t) = 1/Q_e + K_3t \quad (5)$$

where Q_e is the amount of adsorbate at equilibrium per gram of adsorbent (mg g^{-1}), t contact time (min), K_1 , K_2 and K_3 are rate constants of adsorption, respectively, for the pseudo first order (min^{-1}), the pseudo second order (g/mg min) and the second order ($\text{min}^{-1} \text{g/mg}$).

The rate parameter of intraparticle diffusion can be defined as (Weber and Morris, 1963), the initial rate of intra-particle diffusion can be calculated by plotting Q_t against $t^{1/2}$

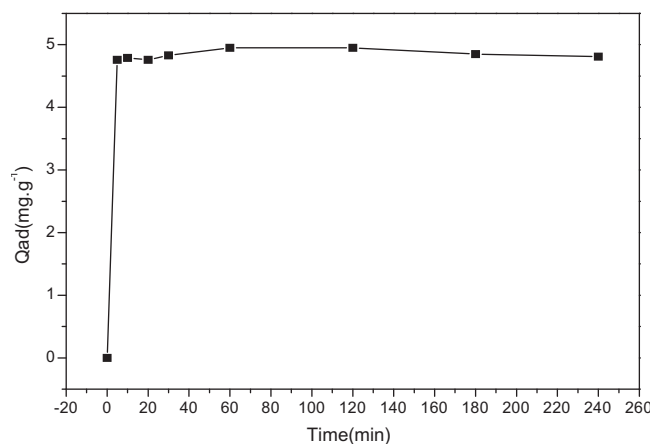


Figure 6 Kinetics of adsorption of DY28 on PTCa (solid quantity: 200 mg, initial dye concentration: 100 mg/L, initial pH, at 298 K, stirring time: 1 min).

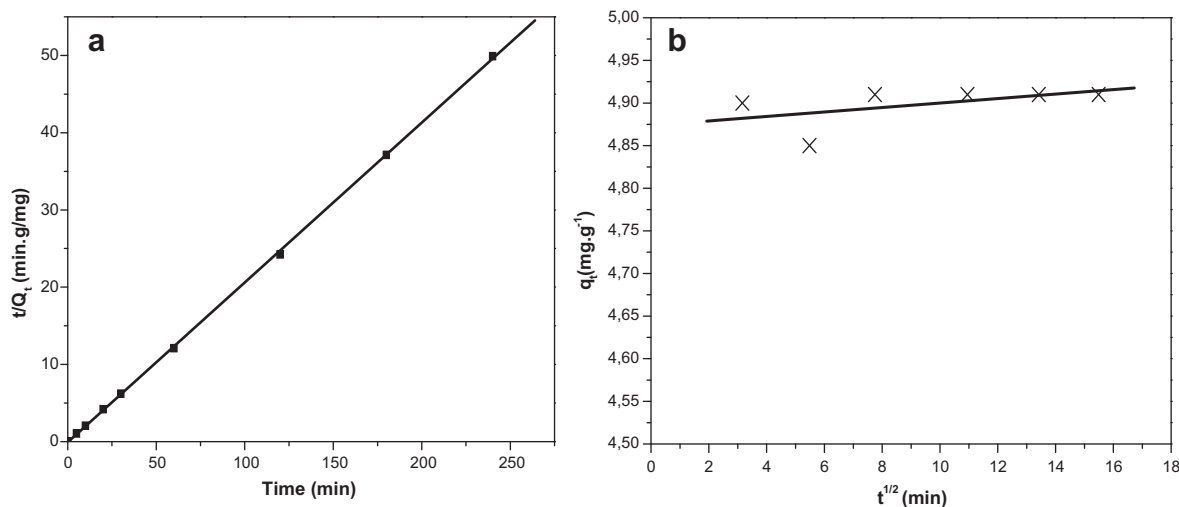


Figure 7 (a) Pseudo second order for adsorption of the DY28 onto PTCa (b) Intraparticle diffusion model for adsorption of the DY28 onto PTCa.

Table 2 The kinetic parameters obtained for Dye adsorption on PTCa.

Second order		Pseudo-second order			Pseudo-first order			Intra-particle diffusion				
Q_e exp ($\text{mg}\cdot\text{g}^{-1}$)	Q_e cal ($\text{mg}\cdot\text{g}^{-1}$)	k_1 ($\text{min}^{-1}\cdot\text{g}/\text{mg}$)	R^2	Q_e cal ($\text{mg}\cdot\text{g}^{-1}$)	k_1 ($\text{g}/\text{mg}\cdot\text{min}^{-1}$)	R^2	Q_e cal ($\text{mg}\cdot\text{g}^{-1}$)	k_1 (min^{-1})	R^2	k_p ($\text{g}\cdot\text{mg}^{-1}\cdot\text{min}^{0.5}$)	C ($\text{mg}\cdot\text{g}^{-1}$)	R^2
4.95	0.161	0.010	0.569	4.834	-0.292	0.999	E-1.80	-14.37E-4	0.571	0.007	4.785	0.433

$$q_t = k_p t^{1/2} + C \quad (6)$$

where, q_t is amount of solute on the surface of the sorbent at time t ($\text{mg}\cdot\text{g}^{-1}$), k_p is the intra-particle rate constant ($\text{mg}\cdot\text{g}^{-1}\cdot\text{min}^{-0.5}$), t is the time (min) and C ($\text{mg}\cdot\text{g}^{-1}$) is a constant that gives an idea about the thickness of the boundary layer.

The intraparticle diffusion model was utilized to determine the rate-limiting step of the adsorption process. According to the model based on the theory proposed by Weber and Morris, if the regression of Q_t versus $t^{1/2}$ was linear and passes through the origin, then adsorption process was controlled by intraparticle diffusion only. The regression was linear, but the plot did not pass through the origin (Fig. 7b), suggesting that adsorption involved intraparticle diffusion, but that was not the only rate-controlling step.

The determination of the different rate constants (Table 2) shows that the model of pseudo second order (Fig. 7a) with a good correlation coefficient ($R^2 = 0.9999$) is the most reliable. Meanwhile, the comparison of calculated values of Q_e with experimental values (Table 2) confirms that the adsorption kinetics are pseudo second order and the dye were adsorbed onto the PTCa surface via chemical interaction. This observation is in agreement with many other studies of kinetics of adsorption of dyes (EL Boujaady et al., 2011; Özcan et al., 2004; Kumar, 2007; EL Haddad et al., 2013).

3.4. Study of adsorption

The adsorption isotherms of DY28 on the phosphate was determined by using 200 mg of adsorbent in contact for 6 h

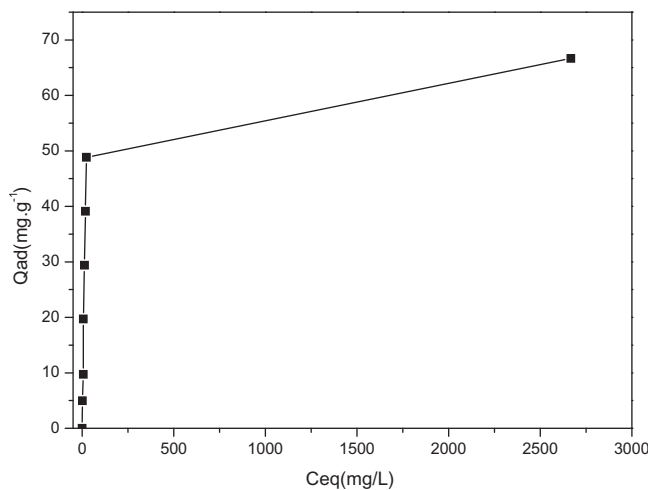


Figure 8 Adsorption isotherms of Direct Yellow 28 by PTCa (solid quantity: 200 mg, stirring time: 1 min, T : 298 K).

with 10 ml of different solutions with a concentration of dye ranging from 100 to 4000 mg/L.

The classical models of Langmuir and Freundlich (Langmuir, 1918; Freundlich, 1906) characterizing the formation of a monolayer are used for their simplicity of implementation. Thus the linearized Langmuir equation (Langmuir, 1918) allowed us to determine the characteristic parameters of adsorption, namely the amount adsorbed at saturation Q_∞ and the constant interaction of adsorbate-adsorbent b .

$$1/Q_{ad} = 1/(bQ_\infty)C_{eq} + 1/Q_\infty \quad (7)$$

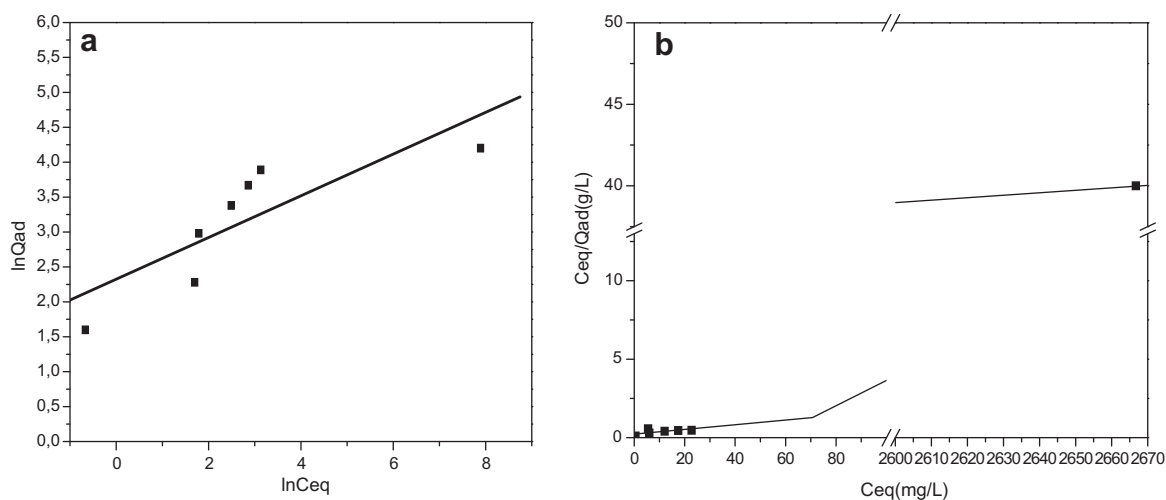


Figure 9 Modeling of adsorption isotherm DY28 from phosphate by (a) Langmuir model and (b) Freundlich model.

Freundlich's law is a purely empirical relationship:

$$Y = aX^m \quad (8)$$

Y is the quantity of substance adsorbed per unit area (or mass) of adsorbent, X : concentration of adsorbate in solution at equilibrium. The parameters a and m characterize the adsorbent–adsorbate pair. The linear transform of this equation is:

$$\text{Log}(Y) = \text{Log}(a) + m\text{Log}(X) \quad (9)$$

The variation of $\text{Log}(Y)$ versus $\text{Log}(X)$ allows to determine a and m . It should be noted that when the amount adsorbed is very low, it is generally Freundlich's law that describes mode of adsorption. For a high recovery rate, it is the law of Langmuir which allows describing this process.

The evolution of the amount adsorbed as a function of its equilibrium concentration in the medium is shown in Fig. 8. It is observed that the amount of absorbed dye increases more quickly for low concentrations in solution and then reaches a plateau; that can be explained by a monolayer adsorption type. The results of modeling of adsorption isotherms by the Langmuir and Freundlich models are shown in Fig. 9. According to the values of correlation coefficients (Table 3), one can say that the Langmuir model appears appropriate only for modeling the adsorption isotherms on apatitic tricalcium phosphate. The adsorption capacity Q_∞ , which is a measure of the maximum adsorption capacity corresponding to complete monolayer coverage was found to be 67.02 mg g^{-1} .

3.5. Effect of pH on the adsorption of dye

The effect of pH was investigated by adding 0.2 g of PTCa into a test tube containing 10 ml of the dye solutions (the initial pH range 4.1–12). The initial dye concentrations of the solutions were fixed at 100 mg/L , for all batch experiments. The

suspension was then stirred for 1 min and the mixtures were placed in a water bath (6 h) at 298 K. Later, the residue was filtered by fritted glass and the pH of supernatant was measured using a pH-meter.

Fig. 10 shows the effect of pH on adsorption of Direct Yellow 28 (DY28) by PTCa, with initial concentration of 100 mg/L and a mass of PTCa of 200 mg. It was observed that the adsorption is highly dependent on the pH of the solution, the adsorption of DY28 decreased with increasing pH and these results can be interpreted by; The point of zero charge pH ZPC of the PTCa is found to be 5.6. Hence, for pH values higher than 5.6, the surface of the PTCa becomes negatively charged and the opposite for pH values lower than 5.6. Moreover, the dye is an anionic molecule; the high adsorption capacity is due to the strong electrostatic interaction between the positively charged surface of PTCa and dye anions. A lower adsorption at higher pH may be due to the abundance of OH^- ions and consequently the ionic repulsion between the negatively charged surface and the anionic dye. Similar behavior has been observed by Mourabet et al., 2012; El Haddad et al., 2013.

3.6. Effect of temperature on adsorption equilibrium

In Fig. 11, we represented the evolution of the amount adsorbed as a function of temperature. There is an increase in temperature, which causes a decrease in the adsorption capacity of dye at equilibrium. The increase in the temperature range 298–318 K, can be explained by the fact that adsorption is an endothermic process.

As reported in the literature, the thermodynamic parameters related to the adsorption process (i.e. the standard free energy change (ΔG), enthalpy change (ΔH) and entropy change (ΔS)) can be calculated using the following equations (Wu, 2007):

Table 3 Values of the constants of Freundlich and Langmuir models.

Langmuir			Freundlich		
Q_∞ (mg/g)	b (l/g)	R^2	m	a (l/g)	R^2
67.02	0.0667	0.9999	0.30	10.2	0.8351

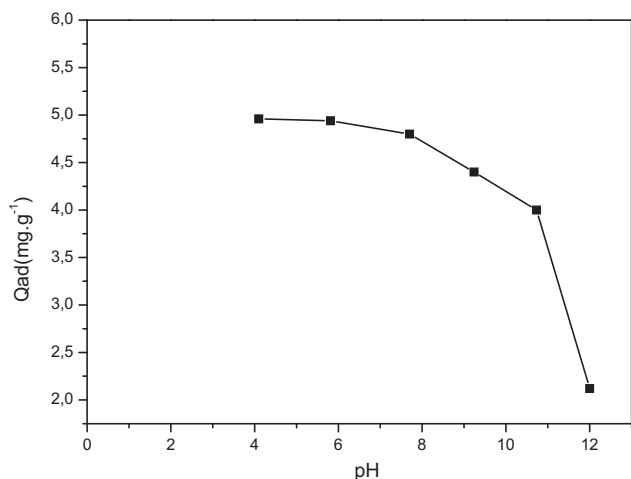


Figure 10 Effect of pH on the adsorption of Direct Yellow 28 on PTCa (solid quantity: 200 mg, initial dye concentration: 100 mg/L, stirring time: 1 min, contact time: 6 h).

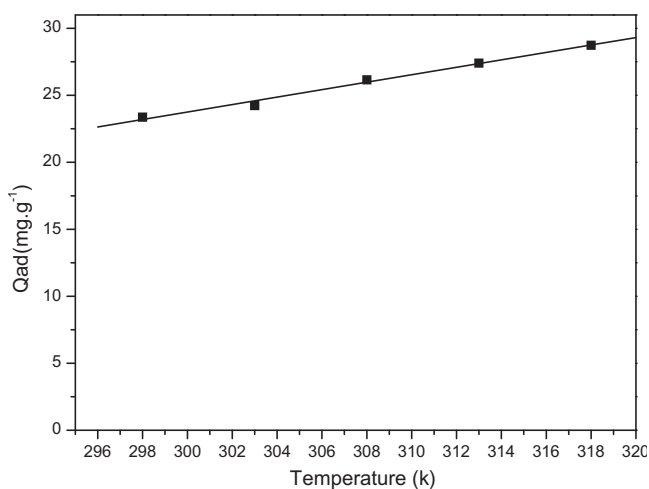


Figure 11 Effect of temperature on the equilibrium adsorption of Direct Yellow 28 on PTCa (Solid quantity: 200 mg, initial dye concentration: 800 mg/L, initial pH, stirring time: 1 min, contact time: 6 h).

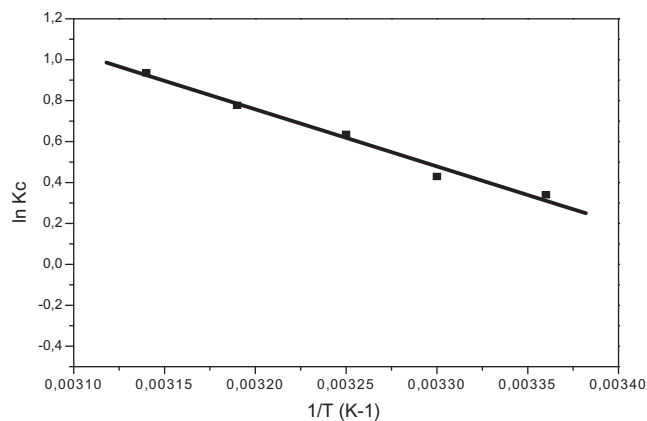


Figure 12 Enthalpy and entropy determination of adsorption of Direct Yellow 28 on PTCa.

Table 4 Thermodynamic parameters of adsorption of the dye from PTCa.

T (K)	ΔG (kJ/mol)	K_c	ΔH (kJ/mol)	ΔS (J/mol k)	R^2
298	-0.8	1.40	23.17	80.45	0.9923
303	-1.21	1.54			
308	-1.61	1.89			
313	-2.01	2.17			
318	-2.41	2.55			

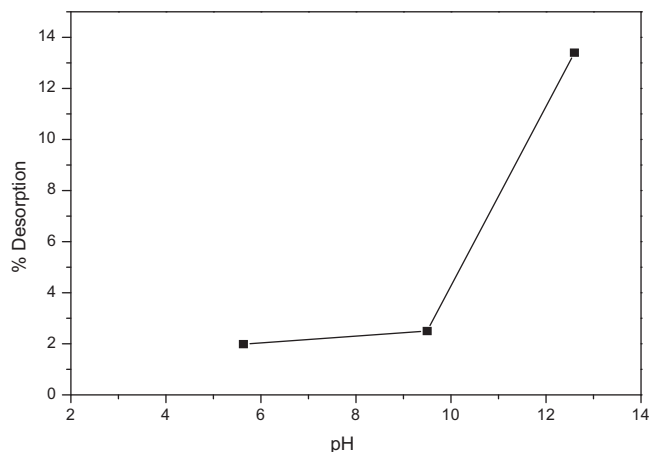


Figure 13 Effect of pH on the desorption of DY28 at 298 K.

$$\Delta G = -RT \ln K_c \quad (10)$$

$$\Delta G = \Delta H - T\Delta S \quad (11)$$

$$\ln K_c = \Delta S/R - \Delta H/RT \quad (12)$$

$$K_c = (C_0 - C_{eq})/C_{eq} \quad (13)$$

where K_c is the Equilibrium constant, ΔG Gibbs free energy (Joule/mole), ΔH Enthalpy (Joule/mole), ΔS Entropy (Joule/mol K), T is the absolute temperature (K), C_0 is the initial concentration of the adsorbate, C_{eq} is the equilibrium concentration, R is the gas constant.

A plot of $\ln K_c$ versus $1/T$ for the initial dye concentration of 800 mg/L was linear (Fig. 12). Values of the ΔH and the ΔS were determined from the slope and intercept of the plot and represented in Table 4. The value of entropy (ΔS) was positive, which indicated the increase in randomness of the ongoing process (Hameed et al., 2007; Mahmoodi et al., 2011). The positive value of the change of ΔH (less than 40 kJ/mol) in this study, which revealed that the adsorption of dye onto PTCa was a physisorption process in nature. Negative values of free energy (ΔG) at each temperature indicated the feasibility and spontaneity of ongoing adsorption. The change in free energy for physisorption and chemisorption is between -20 and 0 kJ/mol and -80 and -400 kJ/mol, respectively (Mahmoodi et al., 2011). The values of ΔG in Table 4 are within the ranges of -20 to 0 kJ/mol indicating that the physisorption is the dominating mechanism. In addition, the values of adsorption (ΔH) obtained in this study (~ 20 kJ/mol) are consistent with hydrogen bond and dipole bond forces for adsorbent (Oepen et al., 1991).

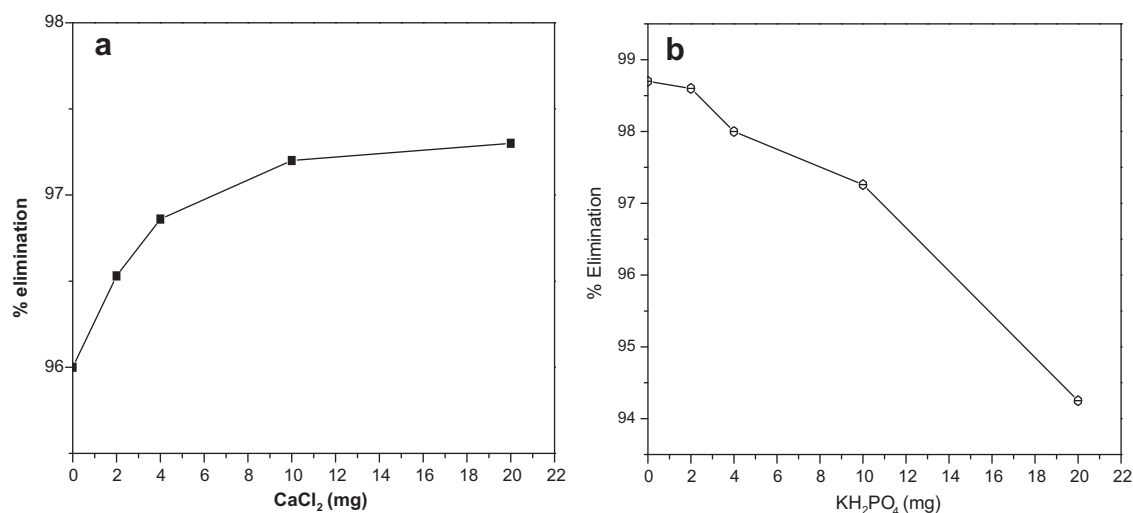


Figure 14 Effect of (a) CaCl₂ and (b) KH₂PO₄ on the adsorption of DY28 ($C = 100$ mg/L).

3.7. Desorption of dye

The adsorption of DY28 was first performed under a dye concentration of 100 mg/L and the adsorbent dose of 0.2 g. The adsorbent was then collected through filtration and air-dried for the desorption experiments. The desorption experiments were carried out by shaking the dye loaded adsorbent in 10 ml of de-ionized water solutions pH = 7.0. The pH of these solutions has been adjusted by either adding NaOH or HCl. After stirring for 5 min at the speed of 1000 trs/min at 298 K, the solid was separated from the solution by filtration through a sintered glass and the dye amount into the solution was determined to calculate removal extent (percent).

$$\text{Desorption (\%)} = (C_{\text{des}}/C_{\text{ad}}) 100 \quad (14)$$

C_{des} and C_{ad} are respectively the desorbed and adsorbed concentration of the dye (mol/L).

The recycling of an adsorbent is the most important aspect for an economical technology. Fig. 13 shows the effect of pH on the desorption of DY28 at 298 K. It was observed that at pH 12.6 desorption efficiency was around 13.4. At pH 12.6 a negatively charged site on the adsorbent disfavors desorption of dye anions due to the electrostatic interaction. At pH 12, a significantly high electrostatic interaction exists between the negatively charged surface of the adsorbent and anionic dye.

3.8. Effect of ions on the adsorption of the dye

Few studies have shown that the addition of ions can cause an increase or decrease of adsorption of dyes (Errais, 2011; Barka, 2008). The adsorption of dyes can also be insensitive to the addition of ions (Baghriche et al., 2008). To clarify the role of phosphate ions and calcium ions on the adsorption phenomena, we added to mixtures of phosphate-dye varying masses going from 2 to 20 mg of calcium chloride CaCl₂ or potassium phosphate KH₂PO₄. The initial dye concentration is 100 mg/L and the mass of apatitic phosphate is 200 mg at initial pH. The results of the study of the adsorption in the presence of calcium ions or phosphate ions are shown in Fig. 14. We note that the ability to remove the dye by the phosphate used decreases in the presence of PO₄³⁻. This decrease is

even more important than the mass of KH₂PO₄ which is high. This is interpreted by the fact that the ions PO₄³⁻ enter in competition with the group $\Phi - \text{SO}_3^-$ of dye molecules to interact with Ca²⁺ ions on the surface of phosphate, a similar result was observed by Mahmoodi et al., 2011 and Bihi et al., 2002. The addition of calcium ions to a solution of Direct Yellow 28 causes an increase in the adsorption capacity.

4. Conclusion

The present study shows that DY28 can be removed from dye bearing effluent in an eco-friendly way using PTCa. The Langmuir model describes satisfactorily the adsorption on PTCa, The percentage of decolorization is 99.49%. X-ray diffraction results showed that, the crystallinity of dye decreased after interaction with DY28 indicates incorporation of the dye into the micropores and macropores of the adsorbent. The results of Fourier transform infrared (FTIR) spectroscopy indicate that the PO₄³⁻ and HPO₄²⁻ groups of the PTCa interact with the dye molecules. The kinetic study shows equilibrium quickly obtained. The kinetics of adsorption is a pseudo-second-order. The adsorption is greatly pH dependent, with a high uptake of dye at low pH and low uptake at high pH. In addition, the maximum adsorption capacity increased from 23.37 to 28.73 mg g⁻¹, when the temperature was increased from 298 to 318 K. Thermodynamic studies indicated that the dye adsorption process by apatitic tricalcium phosphate was physisorption and endothermic in nature.

References

- Baghriche, O., Djebbar, K., Sehili, T., 2008. Kinetic study on adsorption of cationic dye (METHYL GREEN) on activated carbon from aqueous medium. *Sci. Technol.* 27, 57–62.
- Bakan, F., Laçin, O., Sarac, H., 2013. A novel low temperature sol-gel synthesis process for thermally stable nanocrystalline hydroxyapatite. *Powder Technol.* 233, 295–302.
- Barka, N., 2008. Removal of synthetic dyes by adsorption on natural phosphate and photocatalytic degradation on TiO₂ supported. Ph.D. Thesis, Ibn Zohr University, Agadir, Maroc.

- Bihl, N., Bennani-Ziatni, M., Taitai, A., Lebugle, A., 2002. Adsorption of amino acids on calcium phosphates for calcified tissues like carbonates. *Ann. Chim.-Sci. Mat.* 27 (2), 61–70.
- Del Río, A.I., Fernández, J., Molina, J., Bonastre, J., Cases, F., 2011. Electrochemical treatment of a synthetic wastewater containing a sulphonated azo dye. Determination of naphthalenesulphonic compounds produced as main by-products. *Desalination* 273, 428–435.
- Dogan, M., Ozdemir, Y., Alkan, M., 2007. Adsorption kinetics and mechanism of cationic methyl violet and methylene blue dyes onto sepiolite. *Dyes Pigm.* 75, 701–713.
- El Boujaady, H., El Rhilassi, A., Bennani-Ziatni, M., El Hamri, R., Taitai, A., Lacout, J.L., 2011. Removal of a textile dye by adsorption on synthetic calcium phosphates. *Desalination* 275, 10–16.
- El Haddad, M., Mamouni, R., Saffaj, N., Lazar, S., 2012. Removal of a cationic dye – Basic Red 12 – from aqueous solution by adsorption onto animal bone meal. *J. Assoc. Arab Univ. Basic Appl. Sci.* 12, 48–54.
- El Haddad, M., Slimani, R., Mamouni, R., ElAntri, S., Lazar, S., 2013. Removal of two textile dyes from aqueous solutions onto calcined bones. *J. Assoc. Arab Univ. Basic Appl. Sci.* 14, 51–59.
- El Rhilassi, A., El Boujaady, H., Bennani-Ziatni, M., El Hamri, R., Taitai, A., 2011. Adsorption of the L-lysine et de la DL-leucine sur des phosphates de calcium précipités analogues à la partie minérale du tissu osseux. *Ann. Chim.* 36 (1), 45–57.
- El Rhilassi, A., Mourabet, M., El Boujaady, H., Ramdane, H., Bennani-Ziatni, M., El Hamri, R., Taitai, A., 2012. Release of DL-leucine by biomaterials: apatitic calcium phosphates analogous to bone mineral. *J. Mater. Environ. Sci.* 3 (3), 515–524.
- Errais, E., 2011. Reactivity of the natural clays area study of the adsorption of anionic dyes. Ph.D. Thesis, Strasbourg University, Strasbourg, France.
- Freundlich, H.M.F., 1906. Über die adsorption in lasugen. *Z. Phys. Chem. (Leipzig)* 57A, 385–470.
- Hameed, B.H., Ahmad, A.A., Aziz, N., 2007. Isotherms, kinetics and thermodynamics of acid dye adsorption on activated palm ash. *Chem. Eng. J.* 133, 195–203.
- Heughebaert, J.C., 1977. Ph.D. Thesis, Institut National Polytechnique, Toulouse, France.
- Ho, Y.S., McKay, G., 2000. The kinetics of sorption of divalent metal ions onto sphagnum moss peat. *Water Res.* 34, 735–742.
- Ho, Y.S., McKay, G., 1999. Pseudo-second order model for sorption processes. *Process Biochem.* 34, 451–465.
- Iqbal, J., Wattoo, F.H., Wattoo, S.M.H., Malik, R., Tirmizi, S.A., Imran, M., Ghangro, A.B., 2011. Adsorption of acid yellow dye on flakes of chitosan prepared from fishery wastes. *Arab. J. Chem.* 4, 389–395.
- Khataee, A.R., Dehghan, G., 2011. Optimization of biological treatment of a dye solution by macroalgae *Cladophora* sp. using response surface methodology. *J. Taiwan Inst. Chem. Eng.* 42, 26–33.
- Kumar, K.V., 2007. Pseudo-second order models for the adsorption of safranin onto activated carbon: comparison of linear and non-linear regression methods. *J. Hazard. Mater.* 142, 564–567.
- Kyzas, G.Z., Lazaridis, N.K., Mitropoulos, A.Ch., 2012. Removal of dyes from aqueous solutions with untreated coffee Residues as potential low-cost adsorbents: equilibrium, reuse and thermodynamic approach chemical. *Eng. J.* 189–190, 148–159.
- Lagergren, S., 1898. About the theory of so-called adsorption of soluble substances. *Kungliga Svenska Vetenskapsakademiens Handlingar* 24, 1–39.
- Langmuir, I., 1918. The adsorption of gases on plane surfaces of glass, mica and platinum. *J. Am. Chem. Soc.* 40, 1361–1403.
- Lian, L.L., Guo, L.P., Guo, C.J., 2009. Adsorption of Congo red from aqueous solutions onto Ca-bentonite. *J. Hazard. Mater.* 161, 126–131.
- Liao, P., Ismael, Z.M., Zhang, W.B., Yuan, S.H., Tong, M., Wang, K., Bao, J.G., 2012. Adsorption of dyes from aqueous solutions by microwave modified bamboo charcoal. *Chem. Eng. J.* 195–196, 339–346.
- Lin, X.Y., Fan, H.S., Li, X.D., Tang, M., Zhang, X.D., 2005. Evaluation of bioactivity and cytocompatibility of nano hydroxyapatite/collagen composite in vitro. *Key Eng. Mater.* 284, 553–556.
- Maezawa, A., Nakadoi, H., Suzuki, K., Furusawa, T., Suzuki, Y., Uchida, S., 2007. Treatment of dye wastewater by using photocatalytic oxidation with sonication. *Ultrason. Sonochem.* 14, 615–620.
- Mahmoodi, N.M., Hayati, B., Arami, M., Lan, C., 2011. Adsorption of textile dyes on Pine Cone from colored wastewater: kinetic, equilibrium and thermodynamic studies. *Desalination* 268, 117–125.
- Mobasherpour, I., Salahi, E., Pazouki, M., 2012. Comparative of the removal of Pb^{2+} , Cd^{2+} and Ni^{2+} by nano crystallite hydroxyapatite from aqueous solutions: Adsorption isotherm study. *Arab. J. Chem.* 5 (4), 439–446.
- Mohd Salleh, M.A., Mahmoud, D.K., Wan Abdul Karim, A.W., Idris, A., 2011. Cationic and anionic dye adsorption by agricultural solid wastes: a comprehensive review. *Desalination* 280, 1–13.
- Mourabet, M., El Boujaady, H., El Rhilassi, A., Ramdane, H., Bennani-Ziatni, M., El Hamri, R., Taitai, A., 2011. Defluoridation of water using brushite: equilibrium, kinetic and thermodynamic studies. *Desalination* 278, 1–9.
- Mourabet, M., El Rhilassi, A., El Boujaady, H., Bennani-Ziatni, M., El Hamri, R., Taitai, A., 2012. Removal of fluoride from aqueous solution by adsorption on Apatitic Tricalcium phosphate using Box–Behnken Design and desirability function. *Appl. Surf. Sci.* 258, 4402–4410.
- Open, B.V., Kordel, W., Klein, W., 1991. Sorption of nonpolar and polar compounds to soils: processes, measurement and experience with the applicability of the modified OECD-guideline. *Chemosphere* 22, 285–304.
- Özcan, A.S., Erdem, B., Özcan, A., 2004. Adsorption of Acid Blue 193 from aqueous solutions onto Na-bentonite and DTMA-bentonite. *J. Colloid Interface Sci.* 280, 44–54.
- Robinson, T., McMullan, G., Marchant, R., Nigam, P., 2001. Remediation of dyes in textile effluent: a critical review on current treatment technologies with a proposed alternative. *Bioresour. Technol.* 77, 247–255.
- Szygula, A., Guibal, E., Palacin, M.A., Ruiz, M., Sastre, A.M., 2009. Removal of an anionic dye (Acid Blue 92) by coagulation–flocculation using chitosan. *J. Environ. Manage.* 90, 2979–2986.
- Tanyildizi, M.S., 2011. Modeling of adsorption isotherms and kinetics of reactive dye from aqueous solution by peanut hull. *Chem. Eng. J.* 168, 1234–1240.
- Takagi, O., Kuramoto, N., Ozawa, M., Suzuki, S., 2004. Adsorption/desorption of acidic and basic proteins on needle-like hydroxyapatite filter prepared by slip casting. *Ceram. Int.* 30, 139–143.
- Weber, J.R., Morris, J.C., 1963. Kinetics of Adsorption on Carbon from Solution. *Journal of Sanitary Engineering Division ASCE (SA2)89*, 3–60.
- Wei, W., Sun, R., Cui, J., Wei, Z., 2010. Removal of nitrobenzene from aqueous solution by adsorption on nanocrystalline hydroxyapatite. *Desalination* 263, 89–96.
- Wei, W., Wei, Z., Zhao, H., Li, H., Hu, F., 2009. Elimination of the Interference from Nitrate Ions on Oxalic Acid in RP-HPLC by Solid-Phase Extraction with Nanosized Hydroxyapatite. *J. Liq. Chromatogr. Relat. Technol.* 32, 1–19.
- Wu, C.H., 2007. Adsorption of reactive dye onto carbon nanotubes: equilibrium, kinetics and thermodynamics. *J. Hazard. Mater.* 144, 93–100.
- Zhang, J., Wang, L., Zhang, G., Wang, Z., Xu, L., Fan, Z., 2013. Influence of azo dye-TiO₂ interactions on the filtration performance in a hybrid photocatalysis/ultrafiltration process. *J. Colloid Interface Sci.* 389, 273–283.